ENERGY CONSERVING LOCAL DISCONTINUOUS GALERKIN METHODS FOR WAVE PROPAGATION PROBLEMS

Yulong Xing

Computer Science and Mathematics Division, Oak Ridge National Laboratory
and Department of Mathematics, University of Tennessee
Oak Ridge, TN 37831, USA

Ching-Shan Chou

Department of Mathematics, The Ohio State University
Columbus, OH 43221, USA

Chi-Wang Shu

Division of Applied Mathematics, Brown University
Providence, RI 02912, USA

Abstract. Wave propagation problems arise in a wide range of applications. The energy conserving property is one of the guiding principles for numerical algorithms, in order to minimize the phase or shape errors after long time integration. In this paper, we develop and analyze a local discontinuous Galerkin (LDG) method for solving the wave equation. We prove optimal error estimates, superconvergence toward a particular projection of the exact solution, and the energy conserving property for the semi-discrete formulation. The analysis is extended to the fully discrete LDG scheme, with the centered second-order time discretization (the leap-frog scheme). Our numerical experiments demonstrate optimal rates of convergence and superconvergence. We also show that the shape of the solution, after long time integration, is well preserved due to the energy conserving property.

1. **Introduction.** Wave propagation problems arise in science, engineering and industry, and they are significant to geoscience, petroleum engineering, telecommunication, and the defense industry (see [14, 21] and the references therein). Among all the equations describing wave propagation, the constant coefficient wave equation is the simplest one and has been extensively studied. One of the most important properties of the wave equation is the conservation of energy. Experiences reveal that energy conserving numerical methods, which conserve the discrete approximation of energy, are favorable because they are able to maintain the phase and shape of the waves accurately. Numerical methods without this property may result in substantial phase and shape errors after long time integration.

A vast amount of literature can be found on the numerical approximation of the wave equation. All types of numerical methods, including finite difference, finite element, finite volume, spectral methods and integral equation based methods, have

their proponents. Among the partial differential equation techniques, the finite difference method provides an efficient solver, but is usually limited by the shape of the domain. The finite element method can handle complex geometry, but often dissipates energy. Here, we will confine our attention in finite element methods, in particular, discontinuous Galerkin (DG) methods. The DG methods belong to a class of finite element methods using discontinuous piecewise polynomial spaces for both the numerical solution and the test functions. They were originally devised to solve hyperbolic conservation laws with only first order spatial derivatives, e.g. [8, 9, 10, 12, 13]. They allow arbitrarily unstructured meshes, and have compact stencils. Moreover, they easily accommodate arbitrary h-p adaptivity. The DG methods were later generalized to the local discontinuous Galerkin (LDG) methods by Cockburn and Shu to solve convection-diffusion equations [11], motivated by successful numerical experiments from Bassi and Rebay [3] for the compressible Navier-Stokes equations.

Methods for solving the wave equation can be divided into two categories. The first category is to rewrite the wave equation into a first order hyperbolic system. Therefore, various DG methods designed for first order hyperbolic systems can be applied, for example the standard DG method proposed by Cockburn and Shu [10]. High order nodal DG methods for Maxwell's equations of a first order system are proposed in [20]. Space-time DG methods are studied by Falk and Richter in [15], and later by Monk and Richter in [22]. A suboptimal DG method using central fluxes, which is also energy conserving, has been presented in [16] for Maxwell's equations. More recently, Chung and Engquist [5, 6] have proposed an optimal, energy conserving DG method for the wave equation using staggered grids.

The second category of numerical methods is to tackle the second derivatives in the wave equation directly, without introducing more unknowns to reduce the order of the system. Two decades ago, Safjan and Oden [24] introduced a family of unconditionally stable high order Taylor-Galerkin schemes for acoustic and elastic wave propagation. A non-symmetric interior penalty discontinuous Galerkin (IPDG) method has been presented by Rivière and Wheeler in [23]. Later Grote et al. [18, 19] proposed a symmetric IPDG method for the second order equation, which conserves a specifically defined energy. Adjerid and Temimi [1] presented a Galerkin method which uses finite element spaces of continuous functions in space, and discontinuous functions in time, and their method achieves the optimal convergence rate and superconvergence property. Local discontinuous Galerkin method has been applied to the wave equation by Baccouch [2] to study its superconvergence property at the Radau points.

In this paper, we primarily consider the one-dimensional linear wave equation

$$(1) \qquad u_{tt} = u_{xx}, \qquad \text{in } [a,b] \times [0,T],$$

subject to the initial conditions

$$(2) \qquad u(x,0) = u_0(x), \qquad u_t(x,0) = v_0(x).$$

We will consider both the homogeneous Dirichlet boundary conditions

$$(3) \qquad u(a,t) = 0, \qquad u(b,t) = 0,$$

and the periodic boundary condition

$$(4) \qquad u(a,t) = u(b,t).$$

DG method for this problem with the upwind flux has optimal high order accuracy, but is dissipative. On the other hand, DG method with central flux is energy conserving, but is only suboptimal accurate. Usually it is difficult to obtain DG schemes for wave equations which are non-dissipative (energy conserving for the physical energy) and optimal high order accurate, without going to staggered mesh [5, 6] or using penalty with a parameter to adjust [18, 19]. Here, we consider the local discontinuous Galerkin method defined on a single mesh for this linear wave problem. The proposed semi-discrete scheme is shown to be energy conserving. It has the optimal convergence rates in both the energy and L^2 norms, and the upper bound of the errors grows in time only in a linear fashion. This method can achieve superconvergence, towards a particular projection of the exact solution. The order of superconvergence is proved to be $k+3/2$ when piecewise P^k polynomials are used. Coupled with the centered second-order time discretization (the leap-frog method) for the temporal derivatives, we present the fully discrete LDG method, which is explicit in time, and we also show the energy conservation property. To demonstrate the importance of energy conservation, we test an example with long time integration, and the numerical results reveal that our method stays very accurate after long time integration, in contrast to numerical methods without this property. We remark here that since our scheme is non-dissipative, it is more oscillatory than the commonly used upwind (energy-dissipative) DG method when applied to problems with discontinuities. The advantage of energy-conserving methods is to solve smooth wave problems, with the attempt to resolve all waves for long time periods.

This paper is organized as follows. In Section 2, we present the semi-discrete LDG method, and prove its energy conserving property. The optimal error estimates, both in the energy norm and the L^2 norm, are analyzed in Section 3, and therein, the upper bound of errors is proved to grow linearly in time. In Section 4, we prove the superconvergence of the LDG method toward a particular projection of the exact solution. The fully discrete LDG method, with the leap-frog time discretization, and its energy conserving properties are presented in Section 5. Section 6 contains numerical experiments that demonstrate the optimal convergence rates and energy conservation of the proposed LDG method, and a comparison with the IPDG method proposed in [18]. Finally, we give the concluding remarks in Section 7.

2. **Local discontinuous Galerkin discretization.**

2.1. **Notations.** We divide the interval $I = [a, b]$ into N subintervals and denote the cells by $I_j = [x_{j-\frac{1}{2}}, x_{j+\frac{1}{2}}]$ for $j = 1, \cdots, N$. The center of each cell is $x_j = \frac{1}{2}(x_{j-\frac{1}{2}} + x_{j+\frac{1}{2}})$, and the mesh size is denoted by $h_j = x_{j+\frac{1}{2}} - x_{j-\frac{1}{2}}$, with $h = \max_{1 \le j \le N} h_j$ being the maximal mesh size. We assume that the mesh is regular, namely, the ratio between the maximal and the minimal mesh sizes stays bounded during mesh refinement. The piecewise polynomial space V_h^k is defined as the space of polynomials of degree up to k in each cell I_j, that is,

$$(5) \qquad V_h^k = \{v : v|_{I_j} \in P^k(I_j), j = 1, 2, \cdots, N\}.$$

Note that functions in V_h^k are allowed to have discontinuities across element interfaces.

The solution of the numerical scheme is denoted by u_h, which belongs to the finite element space V_h^k. We denote by $(u_h)^+_{j+\frac{1}{2}}$ and $(u_h)^-_{j+\frac{1}{2}}$ the limit values of u_h

at $x_{j+\frac{1}{2}}$ from the right cell I_{j+1} and from the left cell I_j, respectively. We use the usual notations $[u_h] = u_h^+ - u_h^-$ and $\bar{u}_h = \frac{1}{2}(u_h^+ + u_h^-)$ to respectively represent the jump and the mean of the function u_h at the element interfaces. The L^2 norm over the interval I is denoted by $\| \cdot \|$.

2.2. **The LDG method.** In this subsection, we define the semi-discrete LDG method for the wave equation (1), by discretizing the space with the LDG method and leaving the time dependence continuous. First, we write the wave equation into a first order system by substituting u_x with variable q:

$$(6) \qquad u_{tt} = q_x,$$
$$q = u_x.$$

The LDG method for (6) is then formulated as follows: find u_h, $q_h \in V_h^k$, such that

$$(7) \qquad \int_{I_j} (u_h)_{tt} v dx + \int_{I_j} q_h v_x dx - (\hat{q}_h v^-)_{j+\frac{1}{2}} + (\hat{q}_h v^+)_{j-\frac{1}{2}} = 0,$$

$$(8) \qquad \int_{I_j} q_h w dx + \int_{I_j} u_h w_x dx - (\hat{u}_h w^-)_{j+\frac{1}{2}} + (\hat{u}_h w^+)_{j-\frac{1}{2}} = 0,$$

for all test functions v, $w \in V_h^k$. The hatted terms, $\hat{q}_h$ and $\hat{u}_h$, in (7)-(8) are the cell boundary terms obtained from integration by parts, and they are the so-called numerical fluxes. These numerical fluxes are single-valued functions defined on the cell boundaries and should be designed according to guiding principles for different PDEs to ensure numerical stability. Here we use the simple alternating fluxes:

$$(9) \qquad \hat{q}_h = q_h^-, \qquad \hat{u}_h = u_h^+,$$

in which we have omitted the half-integer indices $j + \frac{1}{2}$, as all quantities in (9) are computed at the same points (i.e., the cell interface). In the case of Dirichlet boundary conditions (3), the numerical fluxes (9) at the two boundaries become

$$(10) \qquad (\hat{q}_h)_{\frac{1}{2}} = q_{h,\frac{1}{2}}^+, \qquad (\hat{u}_h)_{\frac{1}{2}} = u(a,t) = 0,$$
$$(\hat{q}_h)_{N+\frac{1}{2}} = q_{h,N+\frac{1}{2}}^-, \qquad (\hat{u}_h)_{N+\frac{1}{2}} = u(b,t) = 0,$$

at the two end boundaries. In the proofs of the following sections, the flux terms at the boundary cells ($j = 1/2$ and $N + 1/2$) will vanish because u vanishes at the boundary, and therefore, we will retain the flux notation of internal cells for simplicity. We remark that the choice of the fluxes (9) is not unique. We can, for example, alternatively choose the numerical fluxes to be

$$(11) \qquad \hat{q}_h = q_h^+, \qquad \hat{u}_h = u_h^-.$$

2.3. **Energy conservation.** As is well-known, the one-dimensional linear wave equation (1) admits an important conserved quantity – the energy, $E = \int_I (u_t^2 + u_x^2) dx$. Experiences show that schemes conserving the discrete analogs of energy often produce approximations that behave better for long time simulation. In this subsection, we will show that the proposed semi-discrete LDG method conserves energy.

Proposition 1. *The (continuous) energy*

$$(12) \qquad E_h(t) = \int_I \left((u_h)_t^2 + q_h^2 \right) dx$$

is conserved by the the semi-discrete LDG method (7)-(8) *for all time.*

Proof. We first take the time derivative of Eq. (8) and choose the test function $w = q_h$ to obtain

$$(13) \qquad \int_{I_j} (q_h)_t q_h dx + \int_{I_j} (u_h)_t (q_h)_x dx - ((u_h)_t^+ q_h^-)_{j+\frac{1}{2}} + ((u_h)_t^+ q_h^+)_{j-\frac{1}{2}} = 0.$$

In Eq. (7), we choose the test function to be $(u_h)_t$:

$$(14) \qquad \int_{I_j} (u_h)_{tt} (u_h)_t dx + \int_{I_j} q_h (u_h)_{tx} dx - (q_h^-(u_h)_t^-)_{j+\frac{1}{2}} + (q_h^-(u_h)_t^+)_{j-\frac{1}{2}} = 0.$$

Adding Eq. (13) to Eq. (14), one obtains

$$\int_{I_j} (u_h)_{tt} (u_h)_t dx + \int_{I_j} q_h (u_h)_{tx} dx - (q_h^-(u_h)_t^-)_{j+\frac{1}{2}} + (q_h^-(u_h)_t^+)_{j-\frac{1}{2}}$$
$$+ \int_{I_j} (q_h)_t q_h dx + \int_{I_j} (u_h)_t (q_h)_x dx - ((u_h)_t^+ q_h^-)_{j+\frac{1}{2}} + ((u_h)_t^+ q_h^+)_{j-\frac{1}{2}} = 0.$$

Using integration by parts on the term $\int_{I_j} q_h (u_h)_{tx} dx$, we get

$$(15) \qquad \int_{I_j} (u_h)_{tt} (u_h)_t dx + \int_{I_j} (q_h)_t q_h dx + (q_h^-(u_h)_t^+)_{j-\frac{1}{2}} - ((u_h)_t^+ q_h^-)_{j+\frac{1}{2}} = 0.$$

If the Dirichlet boundary conditions are used, the flux terms of the boundary cells ($j = 1/2$ and $N + 1/2$) in the above equations will vanish, and therefore, we keep the notation of the internal cells for simplicity.

By summing up Eq. (15) over all cells and using the periodic or Dirichlet boundary conditions, we have

$$\frac{d}{dt} \left(\int_I ((u_h)_t^2 + q_h^2) dx \right) = 0.$$

Therefore the quantity E_h is invariant in time. $\qquad \square$

3. **Error estimate.** In this section, we derive the optimal error estimates for the energy conserving LDG method (7)-(8) proposed in Section 2. The error estimate in the energy norm will be carried out first, and then the analysis will be extended to the L^2 norm. We will also show that these error bounds are both linear in time.

We start by introducing the projections and other notations to be used throughout this paper. The standard L^2 projection of a function $\omega(x)$ with $k+1$ continuous derivatives into space V_h^k is denoted by P_h, i.e.,

$$\int_{I_j} P_h \omega v dx = \int_{I_j} \omega v dx,$$

for any $v \in P^k$ on I_j. In addition, we define $P_h^- \omega$ to be a projection of ω into V_h^k, such that

$$\int_{I_j} P_h^- \omega v dx = \int_{I_j} \omega v dx,$$

for any $v \in P^{k-1}$ on I_j, and

$$(P_h^- \omega)^- = \omega^- \qquad \text{at } x_{j+\frac{1}{2}}.$$

Similarly, the projection $P_h^+ \omega$ is defined as the projection of ω into V_h^k, such that

$$\int_{I_j} P_h^+ \omega v dx = \int_{I_j} \omega v dx,$$

for any $v \in P^{k-1}$ on I_j, and

$$(P_h^+ \omega)^+ = \omega^+ \quad \text{at } x_{j-\frac{1}{2}}.$$

For these projections, it is easy to show (see [7]):

$$(16) \qquad \|\omega^e\| + h\|\omega^e\|_\infty + h^{\frac{1}{2}}\|\omega^e\|_{\Gamma_h} \le Ch^{k+1},$$

where $\omega^e = \omega - P_h\omega$ or $\omega^e = \omega - P_h^\pm \omega$, and Γ_h denotes the set of boundary points of all cells. The constant C depends on the function ω, but is independent of the mesh size h.

Let us denote the errors by

$$(17) \qquad \begin{aligned} e_u &= u - u_h, & \varepsilon_u &= u - P_h^+ u, & \bar{e}_u &= P_h^+ u - u_h, \\ e_q &= q - q_h, & \varepsilon_q &= q - P_h^- q, & \bar{e}_q &= P_h^- q - q_h, \end{aligned}$$

which, from left to right, respectively represent the errors between the exact solution and the numerical solution, the projection errors, and the errors between the numerical solution and the particular projection of the exact solution. Note that the signs of the projection $P_h^\pm$ of u and q in (17) are consistent with the choice of the numerical fluxes in (9). So if the other set of numerical fluxes (11) is chosen, the signs of $P_h^\pm$ in (17) should be changed accordingly.

To obtain the error estimates and the superconvergence property of the proposed LDG method, the projections of the initial conditions for the numerical scheme need to be carefully chosen. Note that we have two initial conditions in (2), one for u and the other for u_t. We take the initial condition $u_h(x,0)$ as $P_h^+ u(x,0) = P_h^+ u_0(x)$, which is consistent with the choice of the numerical fluxes (9). The other initial condition $(u_h)_t(x,0)$ is given by the standard L^2 projection. Thus, we have the following lemma.

Lemma 3.1. *Assume the initial conditions of the LDG scheme* (7)-(8) *are given by*

$$(18) \qquad u_h(x,0) = P_h^+ u(x,0), \qquad (u_h)_t(x,0) = P_h u_t(x,0),$$

there holds the following error estimate

$$(19) \qquad \|\bar{e}_u(0)\| = 0, \qquad \|\bar{e}_q(0)\| \le Ch^{k+1}, \qquad \|(\bar{e}_u)_t(0)\| \le Ch^{k+1},$$

and

$$(20) \qquad \int_{I_j} (e_u)_t(0)v dx = 0, \quad \text{for any } v \in P^k.$$

Proof. Here we only give the proof for the error estimate of $\|\bar{e}_q(0)\|$. All the other results can be obtained similarly.

Subtracting (8) of the LDG method from the weak formulation satisfied by the exact solution q yields

$$(21) \qquad \int_{I_j} e_q w dx + \int_{I_j} e_u w_x dx - (e_u^+ w^-)_{j+\frac{1}{2}} + (e_u^+ w^+)_{j-\frac{1}{2}} = 0,$$

for any test function $w \in V_h^k$. By the properties of the projection P_h^+, we can derive

$$(22) \qquad \int_{I_j} e_q w dx + \int_{I_j} \bar{e}_u w_x dx - (\bar{e}_u^+ w^-)_{j+\frac{1}{2}} + (\bar{e}_u^+ w^+)_{j-\frac{1}{2}} = 0.$$

Since $\bar{e}_u(0) = u_h(0) - P_h^+ u(0) = 0$, we have

$$\int_{I_j} e_q(0) w dx = 0,$$

for any test function $w \in V_h^k$. Taking $w = \bar{e}_q(0)$ yields

$$\|\bar{e}_q(0)\|^2 = \int_I (\bar{e}_q(0))^2 dx = -\int_I \bar{e}_q(0)\varepsilon_q(0) dx \leq \frac{1}{2}\int_I (\bar{e}_q(0))^2 dx + \frac{1}{2}\int_I (\varepsilon_q(0))^2 dx,$$

and therefore,

$$(23) \qquad \|\bar{e}_q(0)\| \leq \left(\int_I (\varepsilon_q(0))^2 dx\right)^{\frac{1}{2}} = O(h^{k+1}).$$

This completes the proof. □

Based on initial conditions (18), we have the following error estimate in the energy norm.

Proposition 2. *Let u and q be the exact solutions of the wave equation* (6)*, and u_h, q_h be the numerical solutions of the semi-discrete LDG method* (7)*-*(8)*, with the numerical fluxes defined in* (9) *and the initial conditions* (18)*. Consider a regular discretization of I and the piecewise polynomial finite element space V_h^k, there holds the following error estimates:*

$$(24) \qquad \|(e_u)_t\| \leq Ch^{k+1}(t+1), \qquad \|e_q\| \leq Ch^{k+1}(t+1),$$

where the constant C depends on $\|u\|_{k+3}$ and $\|u_t\|_{k+2}$.

Proof. By subtracting the LDG method (7)-(8) from the weak formulation satisfied by the exact solutions u and q, we can derive the error equations

$$(25) \qquad \int_{I_j}(e_u)_{tt}v dx + \int_{I_j} e_q v_x dx - (e_q^- v^-)_{j+\frac{1}{2}} + (e_q^- v^+)_{j-\frac{1}{2}} = 0,$$

$$(26) \qquad \int_{I_j} e_q w dx + \int_{I_j} e_u w_x dx - (e_u^+ w^-)_{j+\frac{1}{2}} + (e_u^+ w^+)_{j-\frac{1}{2}} = 0,$$

for all test functions v, $w \in V_h^k$. Using the properties of the projections $P_h^{\pm}$, the error equations are equivalent to

$$(27) \qquad \int_{I_j}(e_u)_{tt}v dx + \int_{I_j} \bar{e}_q v_x dx - (\bar{e}_q^- v^-)_{j+\frac{1}{2}} + (\bar{e}_q^- v^+)_{j-\frac{1}{2}} = 0,$$

$$(28) \qquad \int_{I_j} e_q w dx + \int_{I_j} \bar{e}_u w_x dx - (\bar{e}_u^+ w^-)_{j+\frac{1}{2}} + (\bar{e}_u^+ w^+)_{j-\frac{1}{2}} = 0,$$

Along the same line in the proof of Proposition 1, we first take the time derivative of Eq. (28), choose the test functions $w = \bar{e}_q$, $v = (\bar{e}_u)_t$, and sum up the resulting two equations to get

$$\int_{I_j}(e_u)_{tt}(\bar{e}_u)_t dx + \int_{I_j}(e_q)_t \bar{e}_q dx + (\bar{e}_q^-(\bar{e}_u)_t^+)_{j-\frac{1}{2}} - (\bar{e}_q^-(\bar{e}_u)_t^+)_{j+\frac{1}{2}} = 0.$$

If the Dirichlet boundary conditions are used, the flux terms of the boundary cells ($j = 1/2$ and $N + 1/2$) in the above equations will vanish, and therefore, we keep the notation of the internal cells for simplicity.

By summing up the above equation over all cells and using the periodic or Dirichlet boundary conditions, we have

$$\int_I (e_u)_{tt}(\bar{e}_u)_t dx + \int_I (e_q)_t \bar{e}_q dx = 0$$

Therefore,

$$
\begin{aligned}
\frac{1}{2}\frac{d}{dt}\left(\|(\bar{e}_u)_t\|^2 + \|\bar{e}_q\|^2\right) &= \frac{1}{2}\frac{d}{dt}\int_I \left((\bar{e}_u)_t^2 + \bar{e}_q^2\right)dx \\
&\leq \int_I (\varepsilon_u)_{tt}(\bar{e}_u)_t dx + \int_I (\varepsilon_q)_t \bar{e}_q dx \leq \|(\varepsilon_u)_{tt}\|\|(\bar{e}_u)_t\| + \|(\varepsilon_q)_t\|\|\bar{e}_q\| \\
&\leq C_1 h^{k+1}\|(\bar{e}_u)_t\| + C_2 h^{k+1}\|\bar{e}_q\| \leq Ch^{k+1}(\|(\bar{e}_u)_t\|^2 + \|\bar{e}_q\|^2)^{\frac{1}{2}},
\end{aligned}
$$

which leads to

$$
\frac{d}{dt}\left(\|(\bar{e}_u)_t\|^2 + \|\bar{e}_q\|^2\right)^{\frac{1}{2}} \leq Ch^{k+1}.
$$

Combining this inequality with the property of the initial condition (19), we conclude that

$$
\left(\|(\bar{e}_u)_t\|^2 + \|\bar{e}_q\|^2\right)^{\frac{1}{2}} \leq C(t+1)h^{k+1},
$$

in which the constant C only depends on $\|u\|_{k+3}$ and $\|u_t\|_{k+2}$. Together with the optimal projection error (16), the error estimate (24) follows. $\qquad\square$

Next, we consider the error estimate with respect to the L^2 norm.

Proposition 3. *Let u and q be the exact solutions of the wave equation* (6), *and u_h, q_h be the numerical solutions of the semi-discrete LDG method* (7)-(8), *with the numerical fluxes defined in* (9) *and the initial conditions* (18). *Consider a regular discretization of I and the piecewise polynomial finite element space V_h^k, there holds the following error estimates:*

$$
\text{(29)} \qquad \max_{t \in [0,T]} \|e_u(t)\| \leq Ch^{k+1}(T+1),
$$

where the constant C only depends on the solution u.

Proof. We split $(e_u)_{tt}$ as the summation of $(\bar{e}_u)_{tt}$ and $(\varepsilon_u)_{tt}$ in Eq. (27), and use chain rule in time derivative to obtain

$$
\text{(30)} \qquad
\begin{aligned}
&-\int_{I_j}(\bar{e}_u)_t v_t dx + \int_{I_j}\bar{e}_q v_x dx - (\bar{e}_q^- v^-)_{j+\frac{1}{2}} + (\bar{e}_q^- v^+)_{j-\frac{1}{2}} \\
&= -\int_{I_j}(\varepsilon_u)_{tt} v dx - \frac{d}{dt}\int_{I_j}(\bar{e}_u)_t v dx.
\end{aligned}
$$

For any time $\tau \leq T$, we denote the time integral of the error by

$$
\bar{E}_u(t) = \int_t^\tau \bar{e}_u(s)ds, \quad \bar{E}_q(t) = \int_t^\tau \bar{e}_q(s)ds,
$$

$$
E_q(t) = \int_t^\tau e_q(s)ds, \quad E_q^\varepsilon(t) = \int_t^\tau \varepsilon_q(s)ds.
$$

Taking the integral of Eq. (28) in time, from t to τ, gives

$$
\text{(31)} \qquad \int_{I_j} E_q w dx + \int_{I_j}\bar{E}_u w_x dx - (\bar{E}_u^+ w^-)_{j+\frac{1}{2}} + (\bar{E}_u^+ w^+)_{j-\frac{1}{2}} = 0.
$$

If we choose the test functions to be $v = \bar{E}_u(t)$ and $w = \bar{e}_q(t)$ in (30)-(31), and use the fact that $v_t = -\bar{e}_u(t)$, we have

$$\int_{I_j} (\bar{e}_u)_t \bar{e}_u dx + \int_{I_j} \bar{e}_q (\bar{E}_u)_x dx - (\bar{e}_q^- \bar{E}_u^-)_{j+\frac{1}{2}} + (\bar{e}_q^- \bar{E}_u^+)_{j-\frac{1}{2}}$$

$$= -\int_{I_j} (\varepsilon_u)_{tt} \bar{E}_u dx - \frac{d}{dt} \int_{I_j} (\bar{e}_u)_t \bar{E}_u dx,$$

$$\int_{I_j} E_q \bar{e}_q dx + \int_{I_j} \bar{E}_u (\bar{e}_q)_x dx - (\bar{E}_u^+ \bar{e}_q^-)_{j+\frac{1}{2}} + (\bar{E}_u^+ \bar{e}_q^+)_{j-\frac{1}{2}} = 0.$$

If the Dirichlet boundary conditions are used, the flux terms of the boundary cells ($j = 1/2$ and $N + 1/2$) in the above equations will vanish, and therefore, we keep the notation of the internal cells for simplicity.

Adding up these two equations and summing over all cells, and using the periodic or Dirichlet boundary conditions, one obtains

$$\frac{1}{2} \frac{d}{dt} \left(\|\bar{e}_u\|^2 - \|\bar{E}_q\|^2 \right) = -\int_I (\varepsilon_u)_{tt} \bar{E}_u dx - \frac{d}{dt} \int_I (\bar{e}_u)_t \bar{E}_u dx - \int_I E_q^\varepsilon \bar{e}_q dx$$

$$= -\int_I (\varepsilon_u)_t \bar{e}_u dx - \frac{d}{dt} \int_I (e_u)_t \bar{E}_u dx - \int_I E_q^\varepsilon \bar{e}_q dx.$$

By integrating the inequality from 0 to τ, we get

$$\frac{1}{2} \|\bar{e}_u(\tau)\|^2 - \frac{1}{2} \|\bar{e}_u(0)\|^2 + \frac{1}{2} \|\bar{E}_q(0)\|^2$$

(32)
$$= -\int_0^\tau \int_I (\varepsilon_u)_t \bar{e}_u dx dt + \int_I (e_u)_t(0) \bar{E}_u(0) dx - \int_0^\tau \int_I E_q^\varepsilon \bar{e}_q dx dt,$$

in which the fact $\bar{E}_q(\tau) = \bar{E}_u(\tau) = 0$ is used. By the properties of the projection (16), we have $\|(\varepsilon_u)_t\| = Ch^{k+1}$. Note that

$$E_q^\varepsilon(t) = \int_t^\tau \varepsilon_q(s) ds = \int_t^\tau \left(q(s) - P_h^- q(s) \right) ds = \int_t^\tau q(s) ds - P_h^- \left(\int_t^\tau q(s) ds \right),$$

and therefore we can conclude that $\|E_q^\varepsilon\| = Ch^{k+1}$. Combining with the property of the L^2 projection (20), we have

$$\frac{1}{2} \|\bar{e}_u\|^2(\tau) - \frac{1}{2} \|\bar{e}_u(0)\|^2 + \frac{1}{2} \|\bar{E}_q(0)\|^2$$

$$\leq \left| \int_0^\tau \int_I (\varepsilon_u)_t \bar{e}_u dx dt \right| + \left| \int_0^\tau \int_I E_q^\varepsilon \bar{e}_q dx dt \right|$$

$$\leq \int_0^\tau \|(\varepsilon_u)_t\| \|\bar{e}_u\| dt + \int_0^\tau \|E_q^\varepsilon\| \|\bar{e}_q\| dt$$

$$\leq \tau \max_{t \in [0,\tau]} \|(\varepsilon_u)_t\| \max_{t \in [0,\tau]} \|\bar{e}_u\| + \tau \max_{t \in [0,\tau]} \|E_q^\varepsilon\| \max_{t \in [0,\tau]} \|\bar{e}_q\|$$

$$\leq T \left(\max_{t \in [0,T]} \|(\varepsilon_u)_t\| \max_{t \in [0,T]} \|\bar{e}_u\| + \max_{t \in [0,T]} \|E_q^\varepsilon\| \max_{t \in [0,T]} \|\bar{e}_q\| \right)$$

$$\leq CT \left(h^{k+1} \max_{t \in [0,T]} \|\bar{e}_u\| + (T+1)h^{2k+2} \right)$$

$$\leq C(T^2 + 1)h^{2k+2} + \frac{1}{4} \max_{t \in [0,T]} \|\bar{e}_u\|^2.$$

Since this is true for any $\tau < T$, we have

$$\frac{1}{2}\max_{t\in[0,T]}\|\bar{e}_u\|^2 - \frac{1}{2}\|\bar{e}_u(0)\|^2 + \frac{1}{2}\|\bar{E}_q(0)\|^2 \leq C(T^2+1)h^{2k+2} + \frac{1}{4}\max_{t\in[0,T]}\|\bar{e}_u\|^2.$$

Hence,

$$\frac{1}{4}\max_{t\in[0,T]}\|\bar{e}_u\|^2 + \frac{1}{2}\|\bar{E}_q(0)\|^2 \leq C(T^2+1)h^{2k+2} + \frac{1}{2}\|\bar{e}_u(0)\|^2 = C(T^2+1)h^{2k+2},$$

from which we can conclude

$$\max_{t\in[0,T]}\|e_u(t)\| \leq Ch^{k+1}(T+1).$$

where the constant C only depends on the solution u. $\qquad\square$

4. **Superconvergence.** The superconvergence property of the LDG method is studied in this section. We will prove superconvergence towards a particular projection of the exact solution, with the order $k + 3/2$, in which an increase of $1/2$ over the optimal error estimate of Section 3 can be observed.

To obtain the superconvergence property of the method, two functionals related to the L^2 norm of a function $f(x)$ on I_j, as defined in [4], are needed:

$$\mathcal{B}_j^-(f) = \int_{I_j} f(x)\frac{x-x_{j-1/2}}{h_j}\frac{d}{dx}\Big(f(x)\frac{x-x_j}{h_j}\Big)dx,$$

$$\mathcal{B}_j^+(f) = \int_{I_j} f(x)\frac{x-x_{j+1/2}}{h_j}\frac{d}{dx}\Big(f(x)\frac{x-x_j}{h_j}\Big)dx.$$

Properties of these functionals in the following lemma are essential to the proof of the superconvergence. The proof can be found in [4] and is therefore omitted.

Lemma 4.1. *For any function $f(x) \in C^1$ on I_j, we have*

$$(33) \qquad \mathcal{B}_j^-(f) = \frac{1}{4h_j}\int_{I_j} f^2(x)dx + \frac{f^2(x_{j+1/2})}{4},$$

$$(34) \qquad \mathcal{B}_j^+(f) = -\frac{1}{4h_j}\int_{I_j} f^2(x)dx - \frac{f^2(x_{j-1/2})}{4}.$$

(See [4] for the detailed proof)

We prove the superconvergence of the numerical solution in the following Proposition.

Proposition 4. *Let u and q be the exact solutions of the wave equation (6), and u_h, q_h be the numerical solutions of the semi-discrete LDG method (7)-(8), with the numerical fluxes defined in (9) and the initial conditions (18). Consider a regular discretization of I and the piecewise polynomial finite element space V_h^k, there holds the following error estimate:*

$$(35) \qquad \|\bar{e}_u\| \leq Ch^{k+\frac{3}{2}}(t+1),$$

where the constant C only depends on the solution u.

Proof. In the proof of Proposition 3, we have derived an upper bound for the error term $\|\bar{e}_u(\tau)\|^2$ in Eq. (32). Utilizing the property (20) due to the L^2 projection of the initial condition $(u_h)_t(0)$, Eq. (32) becomes

(36)
$$\frac{1}{2}\|\bar{e}_u(\tau)\|^2 - \frac{1}{2}\|\bar{e}_u(0)\|^2 + \frac{1}{2}\|\bar{E}_q(0)\|^2 = -\int_0^\tau \int_I (\varepsilon_u)_t \bar{e}_u dx dt - \int_0^\tau \int_I E_q^\varepsilon \bar{e}_q dx dt,$$

for any time $\tau \leq T$.

Firstly, we consider the first term on the right-hand side and tackle the term $\bar{e}_u$. We rewrite the error equation (28) as

(37)
$$\int_{I_j} e_q w dx - \int_{I_j} (\bar{e}_u)_x w dx - [\bar{e}_u]w^+\big|_{j-\frac{1}{2}} = 0,$$

by performing integration by parts on the term $\int_{I_j} \bar{e}_u w_x dx$. Define $\bar{e}_u = r_j + d_j(x)(x - x_j)/h_j$ on the cell I_j, where $r_j = \bar{e}_u(x_j)$ is a constant and $d_j(x) \in P^{k-1}$. By choosing the test function w in (37) to be $d_j(x)(x - x_{j-\frac{1}{2}})/h_j$ on I_j, the last term $w^+_{j-\frac{1}{2}}$ will be reduced to 0. Using the definition of $\mathcal{B}_j^-(f)$, one has

$$\int_{I_j} e_q d_j(x)(x - x_{j-\frac{1}{2}})/h_j dx - \mathcal{B}_j^-(d_j(x)) = 0.$$

By Lemma 4.1, this is equivalent to

$$\int_{I_j} e_q d_j(x)\frac{x - x_{j-\frac{1}{2}}}{h_j} dx - \frac{1}{4h_j}\int_{I_j} d_j^2(x) dx - \frac{d_j^2(x_{j+1/2})}{4} = 0,$$

and hence,

(38)
$$\int_{I_j} d_j^2(x) dx \leq 4\int_{I_j} e_q d_j(x)(x - x_{j-\frac{1}{2}}) dx.$$

We define piecewise polynomials $d(x)$ and $\phi_1(x)$, such that $d(x) = d_j(x)$, and $\phi_1(x) = x - x_{j-\frac{1}{2}}$ on I_j. Clearly, $\|\phi_1\|_\infty = \max_j h_j = h$, and Eq. (38) leads to

$$\|d\|^2 \leq 4\|e_q\|\|d\|\|\phi_1\|_\infty \leq 4h\|e_q\|\|d\|.$$

Therefore, by Proposition 2, we have

$$\|d\| \leq 4h\|e_q\| \leq Ch^{k+2}(t+1).$$

Secondly, we repeat similar analysis to the term $\bar{E}_q$ in (36). From Eq. (27), we can derive

$$\int_{I_j} (e_u)_{tt} v dx - \int_{I_j} (\bar{e}_q)_x v dx - [\bar{e}_q]v^-\big|_{j+\frac{1}{2}} = 0.$$

Integrating the above equation in time from t to τ gives

(39)
$$\int_{I_j} ((e_u)_t(\tau) - (e_u)_t(t))v dx - \int_{I_j} (\bar{E}_q)_x v dx - [\bar{E}_q]v^-\big|_{j+\frac{1}{2}} = 0.$$

Similar to the previous analysis, we define $\bar{E}_q = b_j + s_j(x)(x - x_j)/h_j$ on the cell I_j, where b_j is a constant and $s_j(x) \in P^{k-1}$. Choose the test function v in (39) to

be $s_j(x)(x - x_{j+\frac{1}{2}})/h_j$ on I_j, and use the definition of $\mathcal{B}_j^+(f)$ and Lemma 4.1 to obtain

$$\int_{I_j} \left((e_u)_t(\tau) - (e_u)_t(t) \right) s_j(x) \frac{x - x_{j+\frac{1}{2}}}{h_j} dx + \frac{1}{4h_j} \int_{I_j} s_j^2(x) dx + \frac{s_j^2(x_{j-1/2})}{4} = 0.$$

Hence,

$$(40) \qquad \int_{I_j} s_j^2(x) dx \leq 4 \left| \int_{I_j} \left((e_u)_t(\tau) - (e_u)_t(t) \right) s_j(x)(x - x_{j+\frac{1}{2}}) dx \right|.$$

Then we define piecewise polynomials $s(x)$ and $\phi_2(x)$, such that $s(x) = s_j(x)$, and $\phi_2(x) = x - x_{j+\frac{1}{2}}$ on I_j, and finally get

$$\|s\|^2 \leq 4\|(e_u)_t(\tau) - (e_u)_t(t)\| \|s\| \|\phi_2\|_\infty \leq 4h\|(e_u)_t(\tau) - (e_u)_t(t)\| \|s\|.$$

By Proposition 2, we conclude that

$$\|s\| \leq 4\|(e_u)_t(\tau) - (e_u)_t(t)\| \leq Ch^{k+2}(\tau + 1).$$

Lastly, we will use the above results to bound the right-hand side of Eq. (36). By the definition of projections, $(\varepsilon_u)_t$ and E_q^ε are both orthogonal to piecewise constant function, hence

$$\int_I (\varepsilon_u)_t \bar{e}_u dx = \sum_j \int_{I_j} (\varepsilon_u)_t (r_j + d_j(x)(x - x_j)/h_j) dx$$

$$= \sum_j \int_{I_j} (\varepsilon_u)_t d_j(x)(x - x_j)/h_j dx,$$

$$\int_I E_q^\varepsilon \bar{e}_q dx = \sum_j \int_{I_j} E_q^\varepsilon (b_j + s_j(x)(x - x_j)/h_j) dx$$

$$= \sum_j \int_{I_j} E_q^\varepsilon s_j(x)(x - x_j)/h_j dx.$$

Define the function $\phi_3(x) = (x - x_j)/h_j$ on I_j, then $\|\phi_3\|_\infty = \frac{1}{2}$. Therefore,

$$\frac{1}{2}\|\bar{e}_u(\tau)\|^2 - \frac{1}{2}\|\bar{e}_u(0)\|^2 + \frac{1}{2}\|\bar{E}_q(0)\|^2$$

$$\leq \int_0^\tau \left(\|(\varepsilon_u)_t\| \|\phi_3\|_\infty \|d\| + \|E_q^\varepsilon\| \|\phi_3\|_\infty \|s\| \right) dt$$

$$\leq \int_0^\tau \left(Ch^{k+1} \frac{1}{2} Ch^{k+2}(t+1) + Ch^{k+1} \frac{1}{2} Ch^{k+2}(\tau+1) \right) dt$$

$$= \int_0^\tau \left(C(t + \tau + 1)h^{2k+3} \right) dt = C(\tau+1)^2 h^{2k+3}.$$

Combining this inequality with the initial condition (19), and replacing τ by t, we have

$$\|\bar{e}_u(t)\|^2 + \frac{1}{2} \left\| \int_0^t \bar{e}_q(s) ds \right\|^2 \leq C(t+1)^2 h^{2k+3},$$

and in particular

$$\|\bar{e}_u(t)\| \leq C(t+1)h^{k+\frac{3}{2}},$$

where the constant C only depends on the solution u. $\qquad \square$

Although the proofs for both the error estimate in Section 3 and the supercon-vergence in Section 4 are shown with the numerical fluxes (9), the same results hold for the other choice of fluxes (11).

5. **Time discretization.** In order to extend the energy conservation property of the the semi-discrete method to the fully discrete method, it is natural to employ time stepping methods conserving discrete energy. In this paper, we consider the second order leap-frog method for time discretization, which is well-known to be energy conserving.

Let $0 \leq t_0 < t_1 < \cdots < t_N = T$ be a partition of the interval $[0, T]$ with time step $\Delta t_n = t_{n+1} - t_n$. Here uniform time step Δt is used. The fully discrete approximations u_h^n to $u(\cdot, t_n)$ are constructed as follows: for $n = 1, \ldots, N-1$, $u_h^{n+1} \in V_h^k$ is given by

$$(41) \qquad \int_{I_j} \frac{u_h^{n+1} - 2u_h^n + u_h^{n-1}}{\Delta t^2} v dx + \int_{I_j} q_h^n v_x dx - (\hat{q}_h v^-)_{j+\frac{1}{2}} + (\hat{q}_h v^+)_{j-\frac{1}{2}} = 0,$$

$$(42) \qquad \int_{I_j} q_h^n w dx + \int_{I_j} u_h^n w_x dx - (\hat{u}_h w^-)_{j+\frac{1}{2}} + (\hat{u}_h w^+)_{j-\frac{1}{2}} = 0,$$

for all test functions v and w in V_h^k, and the numerical fluxes $\hat{u}_h$, $\hat{q}_h$ are defined as in (9), (10) or (11).

In Proposition 1, we showed the semi-discrete LDG method conserves the con-tinuous energy $E_h(t)$. Along the same line of analysis, we can exhibit the following conserved quantity for the fully discrete method.

Proposition 5. *The solution to the fully discrete leap-frog LDG method* (41)-(42), *conserves the (discrete) energy*

$$(43) \qquad E_h^{n+1} = \left\| \frac{u_h^{n+1} - u_h^n}{\Delta t} \right\|^2 + \left\| \frac{q_h^{n+1} + q_h^n}{2} \right\|^2 - \frac{\Delta t^2}{4} \left\| \frac{q_h^{n+1} - q_h^n}{\Delta t} \right\|^2$$

for all n.

Proof. Suppose the numerical fluxes (9) are used, as the following proof can be car-ried out similarly for fluxes (11). Choose the test function $v = \frac{1}{2}\left(\frac{u_h^{n+1} - u_h^n}{\Delta t} + \frac{u_h^n - u_h^{n-1}}{\Delta t}\right) = \frac{u_h^{n+1} - u_h^{n-1}}{2\Delta t}$ in (41) to obtain

$$(44) \quad \int_{I_j} \frac{u_h^{n+1} - 2u_h^n + u_h^{n-1}}{\Delta t^2} \frac{u_h^{n+1} - u_h^{n-1}}{2\Delta t} dx + \int_{I_j} q_h^n \left(\frac{u_h^{n+1} - u_h^{n-1}}{2\Delta t}\right)_x dx$$
$$- \left((q_h^n)^- \left(\frac{u_h^{n+1} - u_h^{n-1}}{2\Delta t}\right)^-\right)_{j+\frac{1}{2}} + \left((q_h^n)^- \left(\frac{u_h^{n+1} - u_h^{n-1}}{2\Delta t}\right)^+\right)_{j-\frac{1}{2}} = 0.$$

Consider Eq. (42) at time levels t^{n-1} and t^{n+1}, and let the test function w be $\frac{1}{2\Delta t}q_h^n$. Subtracting these two equations yields

$$(45) \quad \int_{I_j} \frac{q_h^{n+1} - q_h^{n-1}}{2\Delta t} q_h^n dx + \int_{I_j} \frac{u_h^{n+1} - u_h^{n-1}}{2\Delta t} (q_h^n)_x dx$$
$$- \left(\frac{(u_h^{n+1})^+ - (u_h^{n-1})^+}{2\Delta t} (q_h^n)^-\right)_{j+\frac{1}{2}} + \left(\frac{(u_h^{n+1})^+ - (u_h^{n-1})^+}{2\Delta t} (q_h^n)^+\right)_{j-\frac{1}{2}} = 0.$$

Adding Eq. (44) to (45) and summing over all cells gives

$$
\int_I \frac{u_h^{n+1} - 2u_h^n + u_h^{n-1}}{\Delta t^2} \frac{u_h^{n+1} - u_h^{n-1}}{2\Delta t} dx + \int_{I_j} \frac{q_h^{n+1} - q_h^{n-1}}{2\Delta t} q_h^n dx
$$

$$
= \int_I \frac{u_h^{n+1} - 2u_h^n + u_h^{n-1}}{\Delta t^2} \frac{u_h^{n+1} - u_h^{n-1}}{2\Delta t} dx + \int_{I_j} \frac{q_h^{n+1} + 2q_h^n + q_h^{n-1}}{4} \frac{q_h^{n+1} - q_h^{n-1}}{2\Delta t} dx
$$

$$
- \int_{I_j} \frac{q_h^{n+1} - 2q_h^n + q_h^{n-1}}{4} \frac{q_h^{n+1} - q_h^{n-1}}{2\Delta t} dx
$$

$$
= \frac{1}{2\Delta t} \left(\left\| \frac{u_h^{n+1} - u_h^n}{\Delta t} \right\|^2 + \left\| \frac{q_h^{n+1} + q_h^n}{2} \right\|^2 - \frac{\Delta t^2}{4} \left\| \frac{q_h^{n+1} - q_h^n}{\Delta t} \right\|^2 \right.
$$

$$
\left. - \left\| \frac{u_h^n - u_h^{n-1}}{\Delta t} \right\|^2 - \left\| \frac{q_h^n + q_h^{n-1}}{2} \right\|^2 + \frac{\Delta t^2}{4} \left\| \frac{q_h^n - q_h^{n-1}}{\Delta t} \right\|^2 \right)
$$

$$
= 0.
$$

Therefore, by the definition of E_h^n in (43), we have $E_h^{n+1} = E_h^n$ for all n, which completes the proof. □

Remark 1. The discrete energy E_h^n can be rewritten as:

$$
(46) \qquad\qquad E_h^{n+1} = \int_I \left(\frac{u_h^{n+1} - u_h^n}{\Delta t} \right)^2 dx + \int_I q_h^{n+1} q_h^n dx,
$$

which is a consistent approximation of the continuous energy (12).

6. **Numerical experiments.** Numerical experiments designed to gauge the performance of our conservative schemes are reported in this section. Attention is given particularly to two issues:

1. Verification of the theoretical results, including a study of the convergence and superconvergence rates.
2. Investigating the long time behavior of our energy conserving scheme, which is also compared with the performance of the energy conserving IPDG method proposed in [19]. This includes a comparison of the errors as a function of time, and the solutions after long time integration.

6.1. **Convergence rates.** In this subsection, we test the order of convergence and superconvergence of the proposed LDG scheme. The results here present the case of uniform meshes, in which the domain is uniformly divided into N cells. Since the second order leap-frog time discretization is employed and our interest is in the effect of the spatial discretization, we determine the time-step by the relation $\Delta t = Ch^2$. This relation guarantees that the error will be dominated by the spatial discretization.

We consider the wave equation

$$
u_{tt} = u_{xx}, \qquad x \in [0, 2]
$$

with initial conditions

$$
u(x, 0) = \sin(\pi x), \quad u_t(x, 0) = 0,
$$

TABLE 1. Numerical errors and orders of LDG method for wave equation with uniform meshes and space P^1.

N	e_u		$\bar{e}_u$		e_q	
	L^2 error	order	L^2 error	order	L^2 error	order
10	1.7099E-02		9.1769E-04		4.2034E-02	
20	4.2397E-03	2.0119	8.8732E-08	13.336	8.1594E-03	2.3650
40	1.0645E-03	1.9938	4.1486E-05	-8.869	5.3769E-03	0.6017
80	2.6556E-04	2.0031	3.8153E-06	3.4428	1.0483E-03	2.3587
160	6.6362E-05	2.0006	8.0124E-08	5.5734	1.3333E-04	2.9750

and a periodic boundary condition $u(0,t) = u(2,t)$ for all $t \geq 0$. This problem was considered in [17] and has the exact solution

$$u(x,t) = \sin(\pi x)\cos(\pi t).$$

We implemented the LDG method with the alternating fluxes (9) and take $\Delta t = 0.01h^2$. Since leap-frog method requires initial conditions for two time steps, we consider Taylor expansion of u at $t = 0$:

$$u(x, \Delta t) = u(x,0) + \Delta t u_t(x,0) + \frac{\Delta t^2}{2}u_{tt}(x,0) + \frac{\Delta t^3}{6}u_{ttt}(x,0) + O(\Delta t^4),$$

and convert the higher derivatives of t to derivatives of x by repeatedly using the wave equation, while u and u_t are given by initial conditions. To obtain the desired order of convergence of u, following the initial conditions (18), we take the projection P_h^+ of $u(x,0)$, and L^2 projection P_h of $u_t(x,0)$; that is, with $u(x,0)$ denoted by u_0 and $u_t(x,0)$ by v_0, to use the initial conditions:

$$u_h^0 = P_h^+ u_0,$$
$$u_h^1 = u_h^0 + \Delta t P_h v_0 + \frac{\Delta t^2}{2}(u_h^0)_{xx} + \frac{\Delta t^3}{6}(P_h v_0)_{xx}.$$

Tables 1 - 3 list the numerical errors and the orders of convergence for P^k spaces, $k = 1, 2, 3$. In each table, the L^2-norm of the errors e_u, $\bar{e}_u$, and e_q at final time $T = 1$ are presented. The $(k+1)$th order for e_u can clearly be observed. However, the order of convergence of $\bar{e}_u$ and e_q may not be fully revealed from the tables. In order to closely examine the order of convergence, we plotted the numerical errors against mesh sizes in Figs. 1-3. The data sets are fitted by straight line in least-squares sense, and the slopes of fitting lines are calculated, as shown atop the figures. Altogether, the slopes of fitting lines for $\bar{e}_u$ are approximately $(k+2)$, and the slopes for e_q are close to $(k+1)$. We would like to mention that, although the superconvergence rate is proved to be of order $k + 3/2$ in Section 4, we can observe the superconvergence of order $k + 2$ in our numerical experiments. The same phenomenon has been observed in [4].

6.2. **Time history of the L^2 error.** In this subsection, we investigate the long time evolution of the L^2 error of the LDG method. An energy conserving IPDG method was proposed in [18], which conserves a specifically defined energy. Here we will compare the performance of these two methods. We consider again the wave equation

$$u_{tt} = u_{xx}, \qquad x \in [0, 2\pi]$$

Table 2. Numerical errors and orders of LDG method for wave equation with uniform meshes and space P^2.

N	e_u		$\bar{e}_u$		e_q	
	L^2 error	order	L^2 error	order	L^2 error	order
10	8.5041E-04		1.3099E-04		4.2597E-03	
20	1.0541E-04	3.0121	3.4527E-06	5.2456	3.7914E-04	3.4899
40	1.3481E-05	2.9670	4.6501E-07	2.8924	6.4696E-05	2.5510
80	1.6795E-06	3.0048	2.3830E-08	4.2864	7.2923E-06	3.1492
160	2.0907E-07	3.0060	7.0408E-10	5.0809	7.2422E-07	3.3319

Table 3. Numerical errors and orders of LDG method for wave equation with uniform meshes and space P^3.

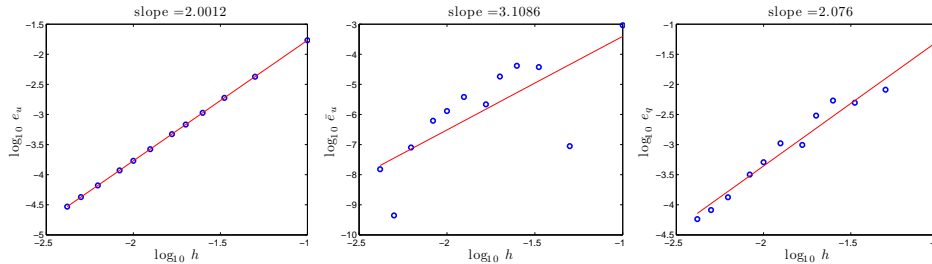| N	e_u		$\bar{e}_u$		e_q	
	L^2 error	order	L^2 error	order	L^2 error	order
10	3.2810e-05		5.4290e-06		2.0398e-04	
20	2.0357e-06	4.0105	1.4383e-07	5.2382	9.8007e-06	4.3794
40	1.2881e-07	3.9822	6.5194e-09	4.4635	9.3343e-07	3.3923
80	8.0431e-09	4.0013	7.0231e-11	6.5365	2.6316e-08	5.1485

Figure 1. Numerical errors, e_u, $\bar{e}_u$ and e_q, with P^1 space are plotted against mesh sizes. Errors are evaluated in L^2 norm and marked by blue circles. Red line is the least square fitting of the data, with the slope of the fitting line displayed on the top of each panel.

with a periodic boundary condition $u(0,t) = u(2\pi, t)$ for all $t \geq 0$, and initial conditions $u(x,0) = e^{\sin x}, u_t(x,0) = -e^{\sin x}\cos x$. This problem has the exact solution $u = e^{\sin(x-t)}$.

The LDG and IPDG methods are implemented with a uniform mesh with N cells, and the leap-frog time discretization, with $\Delta t = 0.6h^2$. For the IPDG method, the interior penalty stabilization parameter is taken to be $40000/\pi$. In order to examine the potential shape difference resulted from long time integration, both methods are run until $T = 1000$, with finite element spaces P^2 and P^3, and $N = 40, 80$, respectively.

In Fig. 4, the time evolution of L^2 errors of both schemes are shown, with red color representing LDG method and blue color for IPDG method, and the errors
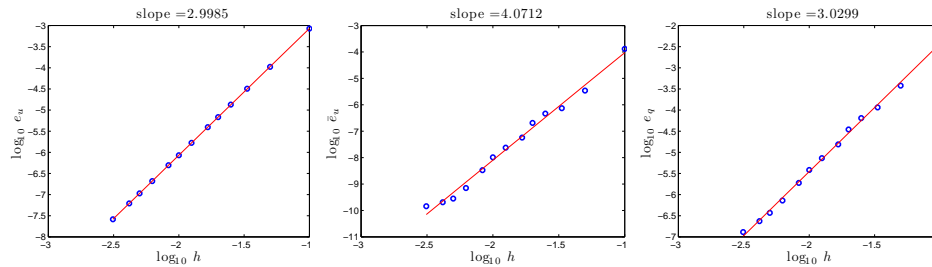
FIGURE 2. Numerical errors, e_u, $\bar{e}_u$ and e_q, with P^2 space are plotted against mesh sizes. Errors are evaluated in L^2 norm and marked by blue circles. Red line is the least square fitting of the data, with the slope of the fitting line displayed on the top of each panel.
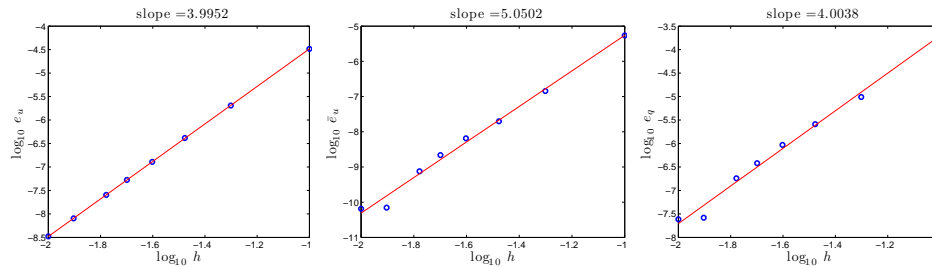

FIGURE 3. Numerical errors, e_u, $\bar{e}_u$ and e_q, with P^3 space are plotted against mesh sizes. Errors are evaluated in L^2 norm and marked by blue circles. Red line is the least square fitting of the data, with the slope of the fitting line displayed on the top of each panel.

are recorded every 10,000 iterations. The L^2 errors of both schemes grow in a linear fashion, but the slope for IPDG method is much larger than that for LDG method, which almost stays as constant and is close to zero. In Fig. 4, the errors are plotted in log scale just for easy visualization. From the figure, one can see that for LDG method, the level of the errors are reduced by refining the mesh from $N = 40$ to $N = 80$, but the mesh refinement does not substantially reduce the errors of IPDG method due to the rapid growth.

It can be observed from Fig. 4 that, up to $T = 1000$, the L^2 error of IPDG method is greater than 10^{-1}, and this large error can easily be visualized by directly comparing the solutions of both methods. Fig. 5 displays the exact solution (red), the solution of LDG method (green) and the solution of IPDG method (blue) at $T = 1000$, for spaces P^2 and P^3 with $N = 40$. It can be seen that solution of LDG method overlaps with the exact solution, while the solution of IPDG method preserves the shape but has a phase shift. A finer mesh with $N = 80$ for IPDG was also tested, and the results look almost identical to Fig. 5, therefore not displayed here. This suggests that a much finer mesh is required to obtain a more accurate numerical solution. We would like to remark that tuning the interior penalty stabilization parameter in IPDG method does result in solutions with different levels of phase shift. However, evident phase error similar to Fig. 5 can still be observed within a large range of the parameter.
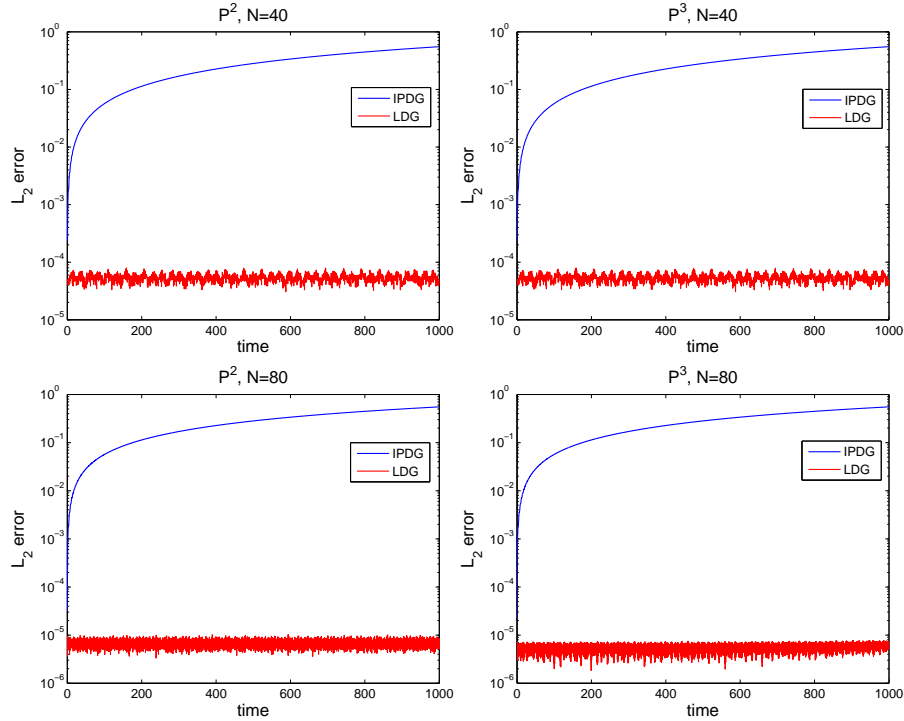
FIGURE 4. Time history until $T = 1000$ of the L^2 error of the numerical approximations obtained from the LDG and IPDG methods with $k = 2, 3$ and a uniform mesh with 40 and 80 cells. The L^2 error on y-axis are presented in log scale.
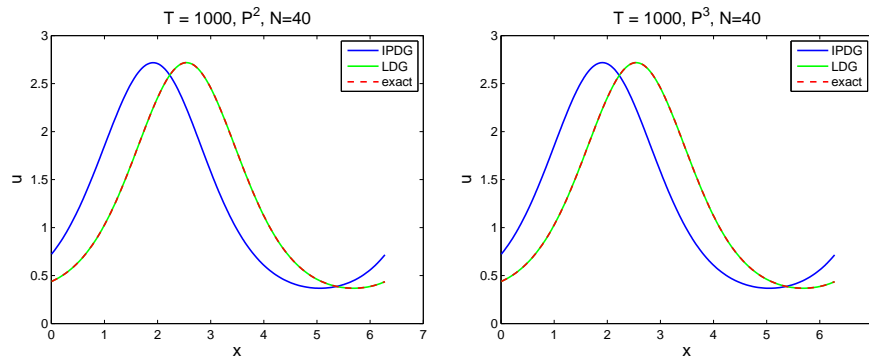

FIGURE 5. Numerical approximations of the wave equation using LDG and IPDG methods. Comparison is made at $T = 1000$ with $k = 2, 3$ and $N = 40$.

7. **Concluding remarks.** In this paper, we developed and analyzed the LDG method for solving the wave equation. We have proved the optimal error estimates, superconvergence towards a particular projection of the exact solution, and its energy conserving property for the semi-discrete formulation. The leap-frog time discretization was used to obtain a fully discrete method, and the fully discrete method is shown to conserve discrete energy. Usually it is difficult to obtain

DG schemes for wave equations which are non-dissipative and optimal high order accurate, without going to staggered mesh [5, 6] or using penalty with a parameter to adjust [18, 19]. Our scheme does not have parameters to tune and is defined on a single mesh. Numerical tests have demonstrated the optimal convergence rates and superconvergence which were proved in this paper. Numerical simulations with long time integration, in comparison with results from IPDG methods, confirmed that energy conservation property is important in order to preserve the phase and shape.

Same techniques in the proofs of this paper can be generalized to variable coefficient problem and also to multi-dimensions, which constitute our current work in progress. Future work also includes designing a higher order time stepping method for the proposed LDG scheme, which conserves energy as the leap-frog discretization. Another direction to pursue is to consider the space-time DG method for the wave propagation problem.

REFERENCES

[1] S. Adjerid and H. Temimi, *A discontinuous Galerkin method for the wave equation,* Computer Methods in Applied Mechanics and Engineering, **200** (2011), 837–849.

[2] M. Baccouch, *A local discontinuous Galerkin method for the second-order wave equation,* Computer Methods in Applied Mechanics and Engineering, **209/212** (2012), 129–143.

[3] F. Bassi and S. Rebay, *A high-order accurate discontinuous finite element method for the numerical solution of the compressible Navier-Stokes equations,* Journal of Computational Physics, **131** (1997), 267–279.

[4] Y. Cheng and C.-W. Shu, *Superconvergence of discontinuous Galerkin and local discontinuous Galerkin schemes for linear hyperbolic and convection diffusion equations in one space dimension,* SIAM Journal on Numerical Analysis, **47** (2010), 4044–4072.

[5] E. T. Chung and B. Engquist, *Optimal discontinuous Galerkin methods for wave propagation,* SIAM Journal on Numerical Analysis, **44** (2006), 2131–2158.

[6] E. T. Chung and B. Engquist, *Optimal discontinuous Galerkin methods for the acoustic wave equation in higher dimensions,* SIAM Journal on Numerical Analysis, **47** (2009), 3820–3848.

[7] P. G. Ciarlet, "The Finite Element Method for Elliptic Problems," Studies in Mathematics and its Applications, Vol. 4, North-Holland Publishing Co., Amsterdam-New York-Oxford, 1978.

[8] B. Cockburn, S. Hou and C.-W. Shu, *The Runge-Kutta local projection discontinuous Galerkin finite element method for conservation laws. IV. The multidimensional case*, Mathematics of Computation, **54** (1990), 545–581.

[9] B. Cockburn, S.-Y. Lin and C.-W. Shu, *TVB Runge-Kutta local projection discontinuous Galerkin finite element method for conservation laws. III. One dimensional systems,* Journal of Computational Physics, **84** (1989), 90–113.

[10] B. Cockburn and C.-W. Shu, *TVB Runge-Kutta local projection discontinuous Galerkin finite element method for conservation laws II: general framework*, Mathematics of Computation, **52** (1989), 411–435.

[11] B. Cockburn and C.-W. Shu, *The local discontinuous Galerkin method for time-dependent convection-diffusion systems,* SIAM Journal on Numerical Analysis, **35** (1998), 2440–2463.

[12] B. Cockburn and C.-W. Shu, *The Runge-Kutta discontinuous Galerkin method for conservation laws. V. Multidimensional systems*, Journal of Computational Physics, **141** (1998), 199–224.

[13] B. Cockburn and C.-W. Shu, *Runge-Kutta discontinuous Galerkin methods for convection-dominated problems,* Journal of Scientific Computing, **16** (2001), 173–261.

[14] D. R. Durran, "Numerical Methods for Wave Equations in Geophysical Fluid Dynamics," Texts in Applied Mathematics, **32**, Springer-Verlag, New York, 1999.

[15] R. S. Falk and G. R. Richter, *Explicit finite element methods for symmetric hyperbolic equations*, SIAM Journal on Numerical Analysis, **36** (1999), 935–952.

[16] L. Fezoui, S. Lanteri, S. Lohrengel and S. Piperno, *Convergence and stability of a discontinuous Galerkin time-domain method for the 3D heterogeneous Maxwell equations on unstructured meshes,* Mathematical Modelling and Numerical Analysis, **39** (2005), 1149–1176.

[17] D. A. French and T. E. Peterson, *A continuous space-time finite element method for the wave equation*, Mathematics of Computation, **65** (1996), 491–506.

[18] M. Grote, A. Schneebeli and D. Schötzau, *Discontinuous Galerkin finite element method for the wave equation*, SIAM Journal on Numerical Analysis, **44** (2006), 2408–2431.

[19] M. Grote and D. Schötzau, *Optimal error estimates for the fully discrete interior penalty DG method for the wave equation*, Journal of Scientific Computing, **40** (2009), 257–272.

[20] J. S. Hesthaven and T. Warburton, *Nodal high-order methods on unstructured grids. I. Time-domain solution of Maxwell's equations,* Journal of Computational Physics, **181** (2002), 186–221.

[21] N. A. Kampanis, J. Ekaterinaris and V. Dougalis, eds., "Effective Computational Methods for Wave Propagation," Numerical Insights, **5**, Chapman & Hall/CRC, Boca Raton, FL, 2008.

[22] P. Monk and G. R. Richter, *A discontinuous Galerkin method for linear symmetric hyperbolic systems in inhomogeneous media*, Journal of Scientific Computing, **22/23** (2005), 443–477.

[23] B. Rivieère and M. F. Wheeler, *Discontinuous finite element methods for acoustic and elastic wave problems,* in "Current Trends in Scientific Computing" (Xi'an, 2002), Contemporary Mathematics, **329**, Amer. Math. Soc., Providence, RI, (2003), 271–282.

[24] A. Safjan and J. T. Oden, *High-order taylor-galerkin and adaptive hp methods for second-order hyperbolic systems: Application to elastodynamics,* Computer Methods in Applied Mechanics and Engineering, **103** (1993), 187–230.

E-mail address: xingy@math.utk.edu

E-mail address: chou@math.ohio-state.edu

E-mail address: shu@dam.brown.edu